

The Effect of Cutting Speed of Nitrogen Laser Cutting on the Surface Texture of SUS 304 Plate

Yanuar Rohmat Aji Pradana*, Raka Afrianto, Chandra Hairat Abdul Rahman, Andoko

Department of Mechanical and Industrial Engineering, Universitas Negeri Malang, Semarang St. No. 5,
Malang, 65145, East Java, Indonesia

*Corresponding author: yanuar.rohmat.ft@um.ac.id

Article history:

Received: 4 May 2023 / Received in revised form: 8 June 2023 / Accepted: 9 June 2023

Available online 15 June 2023

ABSTRACT

The focus of today's machining industry is on how to maintain high productivity and low cost achieved by high tool life during the operation. Laser cutting is considered the right solution because it offers cutting speeds of up to 170000 mm/min through a non-contact process regardless of the workpiece material hardness. The aim of this study is to analyze the effect of cutting speed on the surface texture aspects namely surface roughness, kerf shape, and dross height on the stainless steel 304 plate after laser cutting. The nitrogen laser was utilized with the cutting speed of 400, 1700, and 2000 mm/min and the average roughness (R_a) was then measured using a surface roughness tester. On the other hand, the top, middle, and bottom area of the kerf surface as well as the dross height were analyzed by scanning electron microscopy (SEM). The highest R_a value was resulted at cutting speed of 2000 mm/min with $2.965 \pm 0.05 \mu\text{m}$ while the lowest was at 1400 mm/min with $2.522 \pm 0.16 \mu\text{m}$. In parallel, the R_a was found to be higher when subjected gradually from the top to bottom zone. The kerf surface also proved that the top zone is dominated by the cutting zone, while the middle and bottom zone are characterized by the transition and deformation zone respectively. The width between kerf lines increased when the higher cutting speed was performed. Additionally, the larger dross height was found at the cutting speed of 1400 mm/min with $32.75 \pm 5.21 \mu\text{m}$ and then degraded gradually at the higher cutting speed. The heat input and laser capability in exposing the material thickness are responsible for determining the corresponding surface texture aspects.

Copyright © 2023. Journal of Mechanical Engineering Science and Technology.

Keywords: Cutting speed, dross height, kerf shape, nitrogen laser, stainless steel 304, surface roughness.

I. Introduction

Traces of conventional technology in the railway manufacturing industry experience machining problems in alloy metals, one of which is stainless steel 304 for side wall components of Bangladesh MG (Meter Gauge) Train [1]. It is proven that stainless steel alloy 304 is difficult to be processed with conventional machining due to its high hardness which can reach 145-155 HB [2]. Such properties lead to the accumulation of high amounts of heat and mechanical stress at the edges of the cutting tool at high cutting speed. Increased temperature and cutting force can certainly lead to cutting tool failure [3]. To answer these challenges, non-conventional machining with zero tool-workpiece contact is introduced as the solution. One of the non-conventional machining techniques is laser cutting because it is able to achieve a cutting speed of 170000 mm/min regardless the hardness of the material [4].



Laser cutting is a thermal-based machining technology that uses coherent light as a source for cutting and can be applied to cut many kinds of metal and alloy such as stainless steel, aluminum, copper, etc. The mechanism of laser cutting material disposal is absorption, melting, and vaporization [5]. During vaporization, the material melted by the laser beam is evaporated from the melting area with the help of assisted gas such as nitrogen, oxygen, and atmosphere air. Nitrogen gas is largely applied for cutting stainless steel for many applications [6]. The common dross height achieved by using nitrogen, oxygen, and air are 0.12, 0.27, 0.32 μm , respectively, because nitrogen can exothermically react better in aluminum at 830 °C compared to oxygen and atmospheric air [7].

The parameters to determine the quality of surface texture include cutting speed, laser power, and gas pressure [8], where the key indicators playing an important role in the formation of the surface topography of stainless steel 316 cut is cutting speed [9]. Cutting speed is considered more objective in the range of 1400 to 2000 mm/min against stainless steel 304 thickness 3 mm. The results obtained implied that the regression analysis was successfully applied with an accuracy of 82.7% on surface roughness and 71.67% on kerf width. Based on the results of the ANOVA, the minimum surface roughness was achieved at a cutting speed of 2000 mm/min, laser power of 600 W, and gas pressure of 0.4 bar, while the minimum kerf width was shown at similar level of cutting speed and laser power 600 W but at the gas pressure of 0.5 bar. The surface roughness and kerf width increased as the higher laser power and cutting speed were applied [5]

The other aspects of surface texture besides kerf width are surface roughness, kerf surface, and dross height [10]. The results of cutting abrasive water jet cutting on the top zone of aluminum alloy have better surface quality compared to the bottom zone illustrating that there is a difference in the quality of surface roughness and kerf surface at different thickness zones [11]. Additionally, dross is created due to uneven distribution of vaporization which causes stuck in the bottom zone. Dross is easily found in the bottom zone of stainless steel 316L cutting [9]. Based on these phenomena, surface texture is important to be considered because it affects aesthetics, tribological considerations, corrosion resistance, assembly considerations, and increased fatigue life [12].

Based on the purpose of laser cutting utilization during component manufacturing primarily through machining, it can be expressed as an attempt to achieve predetermined characteristics of product quality within the constraints of equipment cost and time. Rajesh, et al [5] examined and optimized the kerf width and surface roughness of stainless steel 304. However, the study is limited only in a single area of cutting thus it is unable to provide a comprehensive point of view in surface texture aspects under laser cutting parameter variation. In this study, the surface roughness and kerf surface examination were subjected to top, middle, and bottom zones. Additionally, along with the kerf surface, the dross height measurement was performed visually using microscopic observation.

II. Materials dan Method

Stainless steel plate of AISI 304 having dimensions of 1500 x 1000 x 3 mm was prepared for the workpiece material. Based on the material specification, the AISI 304 contained 17.5-19.5% Cr, $\leq 0.07\%$ C, $\leq 1\%$ Si, $\leq 2\%$ Mn, 0.45% P, $\leq 0.015\%$ S, $\leq 0.11\%$ N, and 8-10.5% Ni. The laser machine Trulaser 3060 Fiber was used to cut the plate workpiece. The cutting speeds were set at the value of 1400, 1700, and 2000 mm/min. During the cutting process, a nozzle with a diameter of 1.5 mm at angle of 90° was used under nitrogen exposure. Moreover, the gas pressure, laser power, and stand of distance

were constantly maintained at 0.3 bar, 600 W, and 1.5 mm respectively. The cutting was done for three times of repetition for each cutting speed to ensure the data validity.

After the laser cutting was completed, the surface roughness measurement was conducted using Mitutoyo surface roughness tester based on ISO 4287 standard. The scanning length was taken for 0.8 mm at 3 different locations for each specimen. In parallel, the kerf surface and dross height were analyzed using scanning electron microscope (SEM) according to ASTM C1723 standard with 200 times of magnification. The surface roughness and kerf surface observation were subjected to three different locations based on the material thickness covering top, middle, and bottom zones. Figure 1 shows the location of surface roughness and kerf surface test.

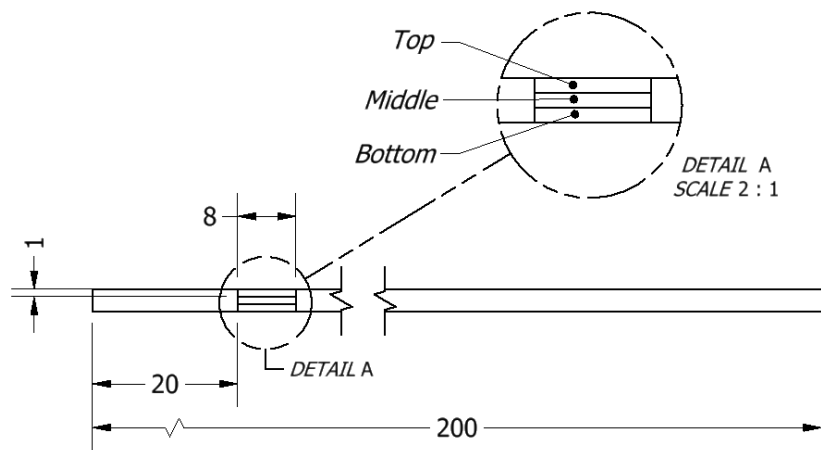


Fig. 1. Surface roughness and kerf surface testing locations. (Unit: mm)

III. Results and Discussion

1. Surface Roughness

The results from surface roughness test are listed in Table 1.

Table 1. Average surface roughness (R_a) with cutting speed variations

Cutting speed (mm/min)	R_a (μm)			Average R_a (μm)
	Top	Middle	Bottom	
1400	1.815	2.695	3.055	2.522 ± 0.05
1700	2.095	2.780	3.170	2.682 ± 0.21
2000	2.170	3.170	3.555	2.965 ± 0.16

Based on Table 1, each cutting speed is divided to top, middle, and bottom. At the cutting speed of 1400 mm / min, the R_a smallest value is in the top zone of 1.815 μm . This value continues to increase in the middle zone of 2.695 μm and the bottom zone of 3.055 μm . Turning to the cutting speed of 1700 mm/min, the top zone R_a is 2.095 μm and the value increases to the bottom zone with R_a of 3.170 μm . Similarly, the cutting speed of 2000 mm/min shows the smaller R_a at top zone with value of 2.170 μm when compared to the middle zone (3.170 μm) and bottom zone (3.555 μm). It indicates that the R_a is higher in a

deeper cutting zone in all cutting speeds. On the other hand, the increase in R_a also occurs when the cutting speed increases. It can be concluded that both cutting speed and location determine the R_a value of the cutting surface. To simplify the data presentation, Figure 2 shows the relationship between cutting speed and R_a in different locations.

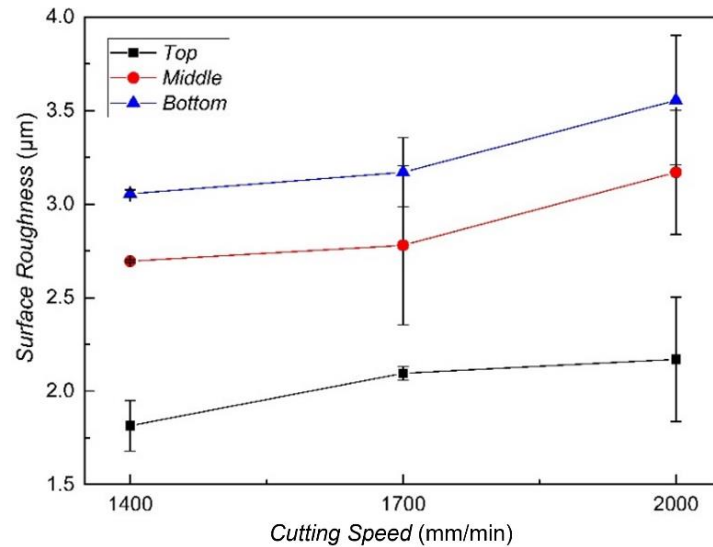


Fig. 2. Relationship between cutting speed and surface roughness (R_a) in different locations.

The main finding in this study is an increase in average surface roughness (R_a) (top, middle, and bottom) along with the increase in cutting speed, as shown in Table 1, compared to previous studies. The previous research reported that the minimum surface roughness is found at the highest cutting speed of 200 mm/min which is contradictory with the results of the current study. It may be because the different characteristics between N laser and CO₂ laser. Moreover, the current study can provide a more complex illustration in the effect of location representing the depth of laser exposure [5].

According to Tosun et al. [11] and Alsoufi et al. [13], the top zone is called smooth zone while middle and bottom zone are called transition and rough zone. The top zone is dominated by better cutting mechanisms because the process of absorption, melting, and vaporization occurs smoothly and quickly. Turning to the middle zone of laser penetration for absorption begins to be disrupted. As a result, remelting takes more time while the nozzle immediately rushes to move due to an increase in cutting speed. Thus, it causes a decrease in the quality received in the R_a of the middle zone. It finally gets worse when moving to the bottom zone. The chance of absorption received by the bottom zone is getting smaller and the cutting process relies on the remaining laser penetration received in the middle zone. At the bottom zone the possible mechanism characterizing the cutting surface is only deformation [11], [13]. This deformation certainly causes the width between kerf lines to be larger when compared to the middle zone, moreover with the top zone [7].

The phenomenon can also be explained from temperature point-of-view. The heat input received by the top surface is theoretically higher than the that at the bottom one inducing a decrease in temperature at the deeper region. The decrease is due to a decrease in laser energy received by the bottom one due to the absorption by the upper material region. The heat transfer process that occurs during cutting is convection. This heat transfer occurs when the melting process forming a pool and penetrates downward (driven by laser power and gravity). Materials in middle zone will melt when the material receives heat due to the

expansion channeled from the top zone. Considering this phenomenon, laser energy is more difficult to penetrate to the bottom zone. The insufficient heat distribution reduce the cutting ability resulting in the enhancement of surface roughness at the deeper zone [14].

The results also implies that the reduction in the volume occurs during material disposal mechanism when the cutting speed increases. By enhancing the cutting speed, the heat received by a unit area of material is reduced due to the shorter time of laser exposure. The decrease in heat reduces formed melting pool [15]. The decrease is well caused by the extensive shear deformation and cutting force generating faster cutting and shortening the kerf width [3]. Thus, the narrower kerf width generates the larger kerf lines in a constant area inducing rough contour and finally measured as a high Ra [7]. The surface roughness results can be a meaningful recommendation for manufacturing industry, such as train company to produce their components (roof, sidewall, end wall, underframe, and bogie) through laser cutting.

2. Kerf Surface

The kerf surface evaluation was done as supplementary evidence in explaining the surface roughness evolution. Microscopic observation by SEM is able to show further the surface texture in an obvious way. Figure 3 shows the kerf surfaces produced by different laser cutting speed in different locations.

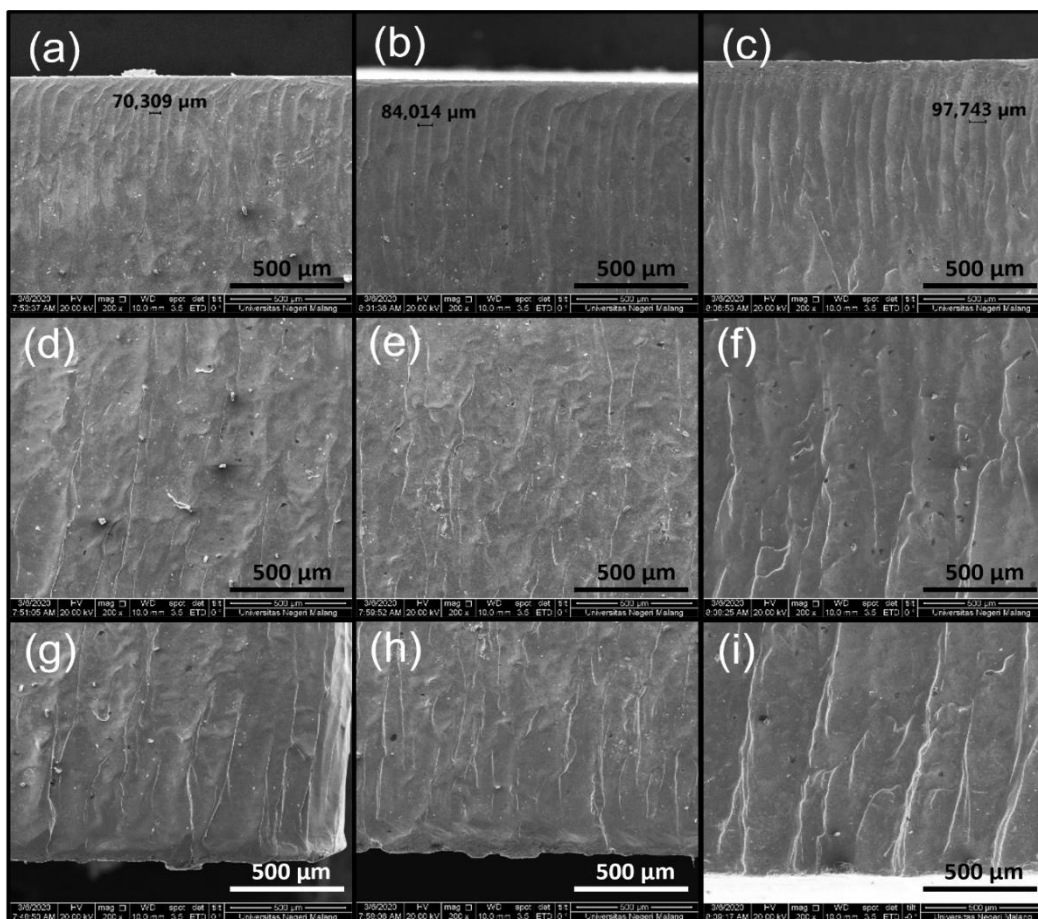


Fig. 3. SEM images showing kerf surfaces of cutting zone generated by the cutting speed of 1400 mm/min at (a) top, (d) middle, (g) bottom; 1700 mm/min at (b) top, (e) middle, (h) bottom zone; and 2000 mm/min at (c) top (f) middle (i) bottom zone.

From Figure 3, it implies that by using nitrogen laser cutting, the enlargement of distances between kerf lines is obvious in all zones (top, middle, and bottom) as the response of cutting speed enhancement. On the other hand, by considering the cutting depth, the distance becomes significantly larger when the observation is conducted at a deeper location. This result is relevant with the previous research on Al 6061-T6 and 7075-T6 cutting using abrasive water jet, where the surface roughness was increased because of cutting speed rise. Moreover, the kerf surface quality at the top zone is far better than the bottom one resulting the lower surface roughness [11].

Top zones as shown in Figure 4 (a), (b), and (c) are called cutting zones. From Figure 4, the increase of cutting speed causes the distance between kerf lines to increase from 70.309; 84.014; and 97.743 μm . The increase of width between kerf lines at the top zone is due to a decrease in heat exposure per area as the cutting speed increases [16]. The laser absorbed material in the top zone becomes unbalanced due to an increase in cutting speed. Increased cutting speed has the effect of increasing cutting force which consequently has an impact on the rise of shear deformation in the cutting zone [3]. The kerf line formed is dominated by fluctuations and oscillations that cause vertical direction due to laminar flow, but still experience tilt due to drag force as cutting speed increases [17]. The increase in cutting speed also induce the increase of the kerf line slope [16].

Turning to the middle zone as presented in Figure 4 (d), (e), and (f), it appears that as the cutting speed increases in this zone there is also a significant change compared to the top zone. The formed kerf line began to disappear, in line with the theory called the transition zone [11]. The decrease in the number of kerf lines is caused by a decrease in energy during the cutting process. The decrease in energy results in the decreasing of areas of melting, fluctuation, and oscillations to focus on forming the same kerf line as the top zone [18]. This is evidenced by the flow change occurring in the middle zone from laminar (top zone) to turbulent (bottom zone) [11]. Increasing cutting speed causes both a decrease in energy and an increase in cutting force causing the width enlargement between kerf lines. Moreover, the kerf valley surface is decreasing as well [19]. The gas pressure ability to evaporate the melt pool drops because the rise of cutting speed limits of the time span of melting and evaporation state [18].

Subsequent exposures to the bottom zone as depicted in Figure 4 (g), (h), and (i) indicates that the kerf surface pattern formed resembles a deformation mark and has been in accordance with the theory called the deformation zone [11]. The increase in the depth of the cutting zone using laser cutting causes more dominant in deformation mechanism. The increase in deformation is caused by a decrease in heat energy limiting the laser penetration to the bottom zone [20]. This results in less laser energy reaching the bottom zone after energy absorption by upper material zone [21]. This deformation certainly causes the width between kerf lines to be enlarged compared to the middle one and moreover with the top zone [7] [19]. This is also influenced by the less ability of gas pressure to evaporate the material as cutting speed increases [18].

3. Dross Height

The amount of dross height data obtained from the test results using the SEM test is divided into the first and second points of each sample. The dross height measurement results are presented in Figure 4 and Table 2.

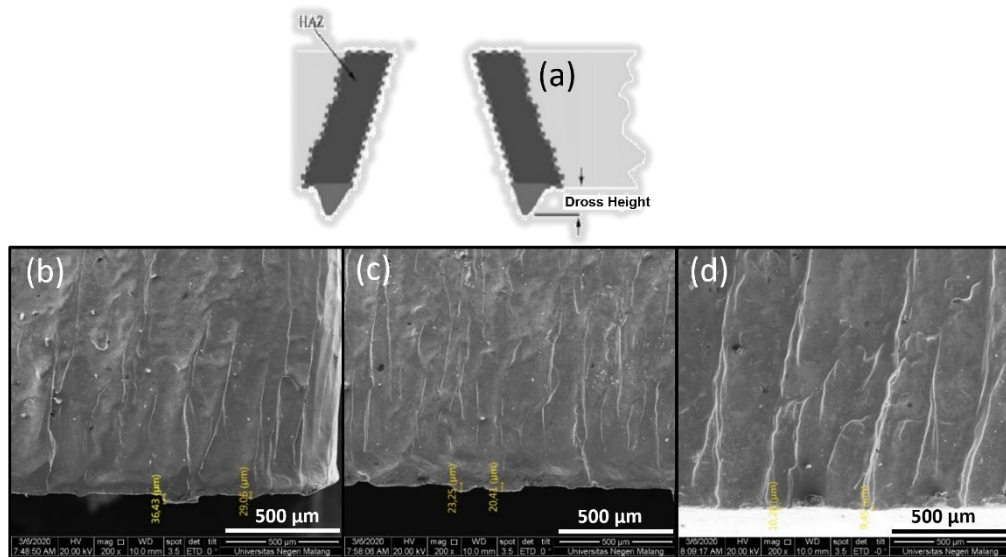


Fig. 4. (a) Illustration of dross height geometry for measurement and SEM images of dross height generated by the cutting speed of (b) 1400, (c) 1700, and (d) 2000 mm/min

Table 2. Dross height measurement results as the function of cutting speed.

Cutting speed (mm/min)	Dross Height (µm)		Average Dross Height (µm)
	First Point	Second Point	
1400	36.43	29.06	32.74 ± 3.68
1700	23.25	20.41	21.83 ± 1.42
2000	10.28	9.45	9.86 ± 0.41

Based on Table 2 and Figure 4, the results show that the average dross height increases as the higher cutting speed is applied. The cutting speed of 1400 mm/min results in the highest dross height with an average of $32.74 \pm 3.68 \mu\text{m}$ while the dross height at a cutting speed of 1700 mm/min averages at $21.83 \pm 1.42 \mu\text{m}$. On the other hand, the cutting speed of 2000 mm/min produces the lowest dross height with an average of $9.86 \pm 0.41 \mu\text{m}$. To simplify the information, the effect of cutting speed on dross height is presented visually in Figure 5.

Based on Figure 5, it can be seen that the dross height data is divided into three cutting speed values. Dross height with the highest value of $36.43 \mu\text{m}$ at a cutting speed of 1400 mm/min and the lowest value of $9.45 \mu\text{m}$ at a cutting speed of 2000 mm/min. There is a decrease in dross height when increasing cutting speed. This can be the effect of cutting speed inducing a lower ability to melt the cutting zone [22], [9]. The heat input of the laser in the cutting zone decreases as the cutting speed enhancement [18]. The loss of heat input affects the formation of melting area volume and fluidity [1]. Heat inputs generally increase at a lower cutting speed, and it decreases at higher cutting speeds. The greater the volume of melting formed, the more difficult it is to be completely evaporated [18]. Based on this outcomes, it is also confirmed by the kerf width formed as the kerf width decreased as the enhancement of cutting speed [19].

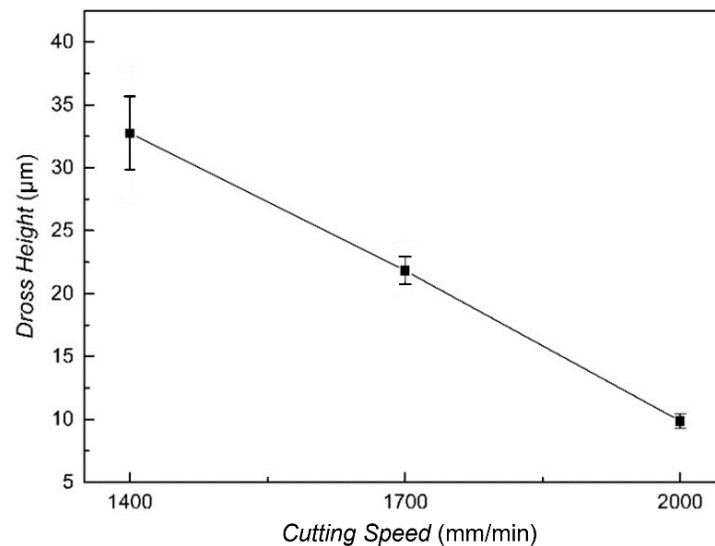


Fig. 5. Average dross height value as a function of laser cutting speed.

The formation of dross also depends on the viscosity, density, and surface tension of the workpiece material. In addition, it also relates to the flow type occurring during cutting where laminar flow takes place at the top zone while turbulent flow locates at the end of the bottom zone. During the cutting process, lower cutting speeds are shown to result in higher material removal. This is because the laser light absorbed by the material stays longer at lower cutting speeds. Along the melting process with low cutting speed, the amount (volume) melting becomes greater than those at the high cutting speed which affects viscosity and fluidity. Therefore, the melt carried out by gas pressure and surface tension material (melting) is lower because of the limited capabilities. The gas pressure not only evaporates the melt, but also generates the shear stress pushing melting area enlargement until the end of specimen bottom zone. When the greater melt pool is formed, the turbulent flow of gas results in ineffective and insufficient vaporization. Thus, the melt solidification is entrapped within the bottom zone as the formation of solidified metal drops. That is why the dross height is higher at low cutting speed than higher cutting speed [18].

The results of this dross height research can be a reference for many automotive manufacturing industries, one of which is the train manufacturing industry. When the sidewall components of the railway train cut by laser cutting requires a low dross height (high quality cutting), a high cutting speed can be selected. It should be underlined that the height of the dross is important to note because it is a consideration for component assembly with other components. The higher the dross height value, the more disruptive the assembly of railway train sidewall components, thus sacrificing the precision of the products. Therefore, it can be concluded that the higher the dross height, the effort of mechanical finishing by grinding process is needed and this consequently increase the cost and time for the train production.

IV. Conclusions

The cutting speed study on the surface texture (surface roughness, kerf surface, and dross height) of SUS 304 on the by nitrogen laser cutting has been successfully conducted. The use of higher cutting speed induced the increase of R_a and the increase is severe at the bottom zone compared to those at the top one. The highest average R_a value was $2.965 \pm$

0.05 μm at a cutting speed of 2000 mm/min and the lowest was $2.522 \pm 0.16 \mu\text{m}$ at a cutting speed of 1400 mm/min. The R_a highest bottom zone value is $3.555 \mu\text{m}$ at a cutting speed of 2000 mm/min and the lowest is $1.815 \mu\text{m}$ at a cutting speed of 1400 mm/min. On the other hand, the rise in cutting speed caused the distance between kerf lines to be widened. Higher cutting speed indicated a lower heat energy and larger cutting force increasing shear deformation at the cutting zone. This characterized the formation of kerf surface from the top zone to the bottom zone. The top zone was dominated by the cutting zone while the middle and bottom zone were mainly dominated by the transition and deformation zone respectively. Finally, increasing cutting speed also resulted in the decrease of dross height. The average value of dross height is highest $32.74 \pm 3.68 \mu\text{m}$ obtained at cutting speed 1400 mm/min and lowest $9.86 \pm 0.41 \mu\text{m}$ at cutting speed 2000 mm/min.

References

- [1] C. Wandera and V. Kujanpää, "Optimization of parameters for fibre laser cutting of a 10 mm stainless steel plate," *Proc. Inst. Mech. Eng. Part B J. Eng. Manuf.*, vol. 225, no. 5, pp. 641–649, 2011, doi: 10.1177/2041297510394078.
- [2] M. A. Chowdhury, D. M. Nuruzzaman, B. K. Roy, S. Samad, R. Sarker, and A. H. M. Rezwan, "Experimental investigation of friction coefficient and wear rate of composite materials sliding against smooth and rough mild steel counterfaces," *Tribol. Ind.*, vol. 35, no. 4, pp. 286–296, 2013.
- [3] R. A. Rahman Rashid, S. Sun, G. Wang, and M. S. Dargusch, "An investigation of cutting forces and cutting temperatures during laser-assisted machining of the Ti-6Cr-5Mo-5V-4Al beta titanium alloy," *Int. J. Mach. Tools Manuf.*, vol. 63, pp. 58–69, 2012, doi: 10.1016/j.ijmachtools.2012.06.004.
- [4] TRUMPF, "TruLaser 3060 fiber," 2020. Available: https://www.trumpf.com/en_INT/products/machines-systems/2d-laser-cutting-machines/trulaser-3030-fiber-3040-fiber-3060-fiber-3080-fiber/
- [5] K. Rajesh, V. V. Murali Krishnam Raju, S. Rajesh, and N. Sudheer Kumar Varma, "Effect of process parameters on machinability characteristics of CO₂ laser process used for cutting SS-304 Stainless steels," *Mater. Today Proc.*, 2019, doi: 10.1016/j.matpr.2019.06.261.
- [6] H. El-Hofy, *Machining processes, Conventional and Nonconventional*. United States of America: CRC Press Taylor & Francis Group, 2014.
- [7] F. Farrokhi, S. E. Nielsen, R. H. Schmidt, S. S. Pedersen, and M. Kristiansen, "Effect of Cut Quality on Hybrid Laser Arc Welding of Thick Section Steels," *Phys. Procedia*, vol. 78, no. August, pp. 65–73, 2015, doi: 10.1016/j.phpro.2015.11.018.
- [8] W. Chuaiphan and L. Srijaroenpramong, "Optimization of gas tungsten arc welding parameters for the dissimilar welding between AISI 304 and AISI 201 stainless steels," *Def. Technol.*, vol. 15, no. 2, pp. 170–178, 2019, doi: 10.1016/j.dt.2018.06.007.
- [9] X. Sun, X. Wei, Z. Li, J. Zhang, and Y. Wang, "Study on process technology and surface integrity of 316L cardiovascular stents by fiber laser wet cutting," *Int. J. Adv. Manuf. Technol.*, 2019, doi: 10.1007/s00170-018-03252-2.
- [10] N. B. Dahotre and S. P. Harimkar, *Laser Fabrication and Machining of Materials*, vol. 53, no. 9. New York: Springer, 2008. doi: 10.1017/CBO9781107415324.004.

- [11] N. Tosun, I. Dagtekin, L. Ozler, and A. Deniz, "Abrasive waterjet cutting of aluminum alloys: Workpiece surface roughness," *Appl. Mech. Mater.*, vol. 404, pp. 3–9, 2013, doi: 10.4028/www.scientific.net/AMM.404.3.
- [12] M. Kuttolamadom, S. Hamzehlouia, and L. Mears, "Effect of machining feed on surface roughness in cutting 6061 aluminum," *SAE Tech. Pap.*, vol. 3, no. 1, pp. 108–119, 2010, doi: 10.4271/2010-01-0218.
- [13] M. S. Alsoufi, D. K. Suker, A. S. Alsabban, and S. Azam, "Experimental Study of Surface Roughness and Micro-Hardness Obtained by Cutting Carbon Steel with Abrasive WaterJet and Laser Beam Technologies," vol. 4, no. 5, pp. 173–181, 2016, doi: 10.12691/ajme-4-5-2.
- [14] S. Sohail Akhtar, B. Sami Yilbas, and E. Bayraktar, "Thermal stress distributions and microstructure in laser cutting of thin Al–Si alloy sheet," *J. Laser Appl.*, vol. 25, no. 4, p. 042006, 2013, doi: 10.2351/1.4807081.
- [15] S. Sun, M. Brandt, J. E. Barnes, and M. S. Dargusch, "Experimental investigation of cutting forces and tool wear during laser-assisted milling of Ti-6Al-4V alloy," *Proc. Inst. Mech. Eng. Part B J. Eng. Manuf.*, vol. 225, no. 9, pp. 1512–1527, 2011, doi: 10.1177/0954405411411608.
- [16] L. D. Scintilla and L. Tricarico, "Experimental investigation on fiber and CO₂ inert gas fusion cutting of AZ31 magnesium alloy sheets," *Opt. Laser Technol.*, vol. 46, no. 1, pp. 42–52, 2013, doi: 10.1016/j.optlastec.2012.04.026.
- [17] D. Teixidor, J. Ciurana, and C. A. Rodriguez, "Dross formation and process parameters analysis of fibre laser cutting of stainless steel thin sheets," *Int. J. Adv. Manuf. Technol.*, vol. 71, no. 9–12, pp. 1611–1621, 2014, doi: 10.1007/s00170-013-5599-0.
- [18] L. D. Scintilla, D. Sorgente, and L. Tricarico, "Experimental investigation on fiber laser cutting of Ti6Al4V thin sheet," *Adv. Mater. Res.*, vol. 264–265, pp. 1281–1286, 2011, doi: 10.4028/www.scientific.net/AMR.264-265.1281.
- [19] B. S. Yilbas, M. M. Shaukat, and F. Ashraf, "Laser cutting of various materials: Kerf width size analysis and life cycle assessment of cutting process," *Opt. Laser Technol.*, vol. 93, pp. 67–73, 2017, doi: 10.1016/j.optlastec.2017.02.014.
- [20] M. Harničárová *et al.*, "Predicting residual and flow stresses from surface topography created by laser cutting technology," *Opt. Laser Technol.*, vol. 52, pp. 21–29, 2013, doi: 10.1016/j.optlastec.2013.03.024.
- [21] X. Cheng, L. Yang, M. Wang, Y. Cai, Y. Wang, and Z. Ren, "Laser beam induced thermal-crack propagation for asymmetric linear cutting of silicon wafer," vol. 120, no. August, 2019, doi: 10.1016/j.optlastec.2019.105765.
- [22] E. Haddadi, M. Moradi, A. Karimzad Ghavidel, A. Karimzad Ghavidel, and S. Meiabadi, "Experimental and parametric evaluation of cut quality characteristics in CO₂ laser cutting of polystyrene," *Optik (Stuttg.)*, vol. 184, no. February, pp. 103–114, 2019, doi: 10.1016/j.ijleo.2019.03.040.